AN ALGORITHM OF A FREEFORM SURFACES MEASUREMENT ADJUSTMENT USING A SPECIFICATION OF THE WORKPIECE COORDINATE SYSTEM LOCATION

Ján Buša[1], Ján Buša Jr.[1], Miroslav Dovica[2], Michal Fabian[2], Peter Ižol[2], Stanislav Honus[3]

[1] Faculty of Electrical Engineering and Informatics, Technical University of Košice, Letná 9, 042 00, Košice, Slovak Republic, e-mail: jan.busa@tuke.sk

[2] Faculty of Mechanical Engineering, Technical University of Košice, Letná 9, 042 00, Košice, Slovak Republic, e-mail: miroslav.dovica@tuke.sk; michal.fabian@tuke.sk; peter.izol@tuke.sk

[3] VŠB – Technical University of Ostrava, 17. listopadu 15/2172, 708 33 Ostrava – Poruba, Czech Republic

ABSTRACT

A difficulty of freeform surfaces evaluations lies in a setup of a coordinate measuring system in general, when it is not possible to use the standard system of alignment by a point, a line, and a surface. An algorithm for the measurement adjustment using a small workpiece coordinate system movement and rotation to achieve a smaller least square error of the produced surface for a given freeform surface defined by the function of two variables is considered. The algorithm uses the Newton method for calculation of the orthogonal distance of a measured point to a given surface and also for minimization of the sum of the distance squares. Numerical results for an example are given.

Keywords: freeform surface, cloud of points, Nelder-Mead method, Newton method.

INTRODUCTION

Implementation of CAx systems into the process of design, production, and measurement in the mechanical engineering had a considerable impact on the product design, mainly in the consumer goods and automotive industries. CAx systems development is still ongoing and allows creating freeform surfaces as well as precise surfaces that are empirically described by mathematical equations. The form surface defined by mathematical expression enables us to obtain the exact shape, which is subsequently produced on a CNC machine. This whole process affects the quality of machined surfaces.

Freeform surfaces are still considered to be artists' not engineers' work. The paradox is that mass production of freeform surfaces were enabled mainly by engineering. In spite of these, the freeform surfaces are around us more and more.

The freeform surfaces have become the reality of series production in aviation, automotive and consumer goods industry at the time when modern optoelectronic scanning devices and CAD systems entered the re-engineering process. This issue was elaborated by Ohara and Higashi already in 1983 [1], Mehrad, Xue, and Gu in [2], Sitnik and Blaszczyk in [3], Garbacz et. al. in [21] or Molnár et. al. in [19]. Modern scanners can deliver numerical information of the product geometry in a form of x, y, z coordinates – so-called clouds of points.

These can be then loaded into CAD systems, triangulated and after making cross cuts of this triangulated data we can identify the cross section curves. This allows us to define smooth shape surfaces.

Reverse engineering process is a subject of interest to engineers and scientists and is being constantly improved. Oe, Shizuki, and Tanaka discuss this topic in [4] and Kruth and Kersten

Fig. 1. Sine (above) and cosine (below) function in the CATIA Law Editor

in [5]. The process is completed when perfectly smooth surfaces are created and subsequently forwarded to a toolroom. Wu, Yang, and Guo deal with it in [6]. Ochiai and Sekiya discussed about generation of freeform surface in CAD for dies in 1995 in [7]. About CNC machining freeform surfaces discuss Lo in [8], Wei and Lin in [9], and Sacharow et. al. in [10].

The accuracy of workpieces of complex freeform surfaces is achieved by tolerancing, producing, and metrology of workpieces. The tolerance zone is defined by form tolerances, their orientation, and location on the workpieces. Tolerances for complex form surfaces are specified by line profile tolerance or surface profile tolerance. These tolerances control form or combination of size, form, orientation, and location. This issue was elaborated by Kráľ and Kráľ [22]. In a machining process, the impact of machining parameter settings on the final surface quality will be studied. For geometry verification of the complex form surfaces the coordinate measurements will be used. The measurement area will in CATIA V5 be modeled by equations. The data of machined surface will be obtained through 3D measurement.

The issue of measurement and obtaining the shape will be solved by the contact measurement using contact scanners or without contact via optoelectronic scanners. This issue is addressed by Fanf and Zhang Qiu in [11] and Debski et. al. in [20]. Lee and Shiou [12] and Kale and Gurumoorthy [13], Fedorko et. al [23] and Kulka et. al [24] deal with the issue of freeform surface measurement.

WORKPIECE MANUFACTURING AND QUALITY CONTROL

This work discusses the creation of surface defined by limiting curves that are set by sine profile of limiting curves on one side and cosine profile of limiting curve on other. This shape simulated freeform surface defined by mathematical functions (sine and cosine) in CATIA. This model was applied when producing the gauge called SC01 that was consequently measured. Accordingly, second model was designed. Its basic shape was defined by cloud of points generated in MATLAB. Such cloud was approximated by surface that was produced and named MR02. This model was measured, too.

Mathematical definition of surfaces in CATIA V5

For this research, it was necessary to produce two artifacts. As it was already mentioned, the first artifact was defined by two limits defined by mathematical function on which the surface is put using Multisection surface command in CATIA V5. Firstly, it was necessary to input parameters
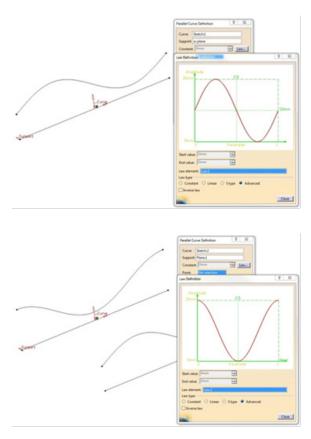

Fig. 2. Definition of sine (above) and cosine (below) curves in CATIA V5
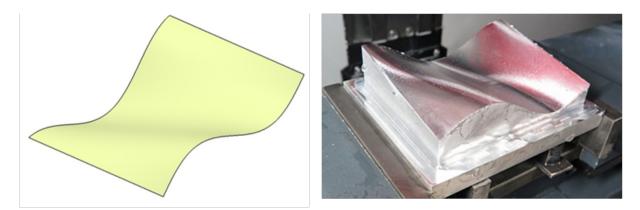
Fig. 3. Final surface defined by the sine and cosine functions (left) and part produced by a milling machine (right)

and equations. Equations were defined in CATIA Law Editor (Fig. 1).

Curves defined by sine in Eq. (1) and cosine functions in Eq. (2) created limits to create the surface of sample SC01 (Fig. 2).

The inserted functions are of the form:

$$z = 15 + 10 \cdot \sin \frac{2\pi x}{100} \qquad (1)$$

$$z = 15 + 10 \cdot \cos \frac{2\pi x}{100} \qquad (2)$$

The final virtual freeform surface is shown in Figure 3. Furthermore, it was used to generate CNC program for production of artifact on 3D milling machine EMCO Concept Mill 155.

Surface defined by cloud of points in CATIA V5

The second surface model was designed using cloud of points generated in MATLAB according to Eq. (16). This cloud was then imported in the environment Digitized Shape Editor in CATIA V5. Final form of the surface was cre-

ated by putting the surface onto the cloud using command Power Fit (Fig. 4). As such, the surface MR02 was created. The second artifact was also produced using 3D CNC Milling Machine.

Artifact manufacturing

On the basis of the surface model, CNC data were generated for production samples that were afterward subjected to measurements. The artifacts were milled into aluminum and machined by ball end tool on EMCO Concept Mill 155 milling machine. Machining strategy is in transversal direction when the main movement of the tool is in the width direction of the workpiece (*y*-axis) (Fig. 5 a) using the isoparametric machining strategy (Fig. 5 b). At first we rough the stock of material and after that make finishing operation (Fig. 6). The distance between two successive toolpaths was recalculated on the basis of a height inequality value setting (Scallop Height), (see Fig. 7). The maximum Scallop Height value was set to 0.001 mm.
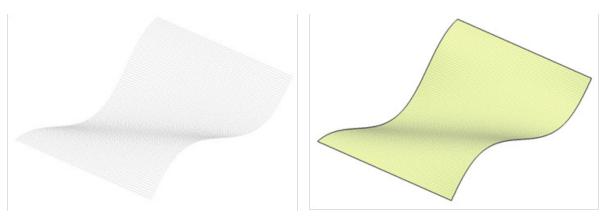

Fig. 4. Cloud of points (left) import to CATIA and surface based on this cloud of points (right)
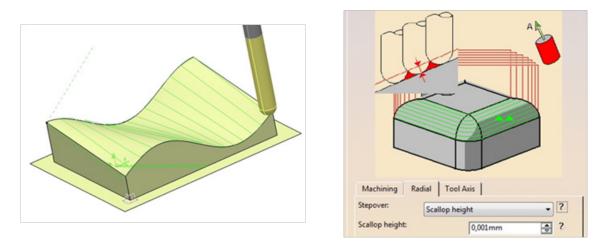
Fig. 5. Definition of machining strategy - movement of the tool (left) and parameters of isoparametric machining strategy (right)
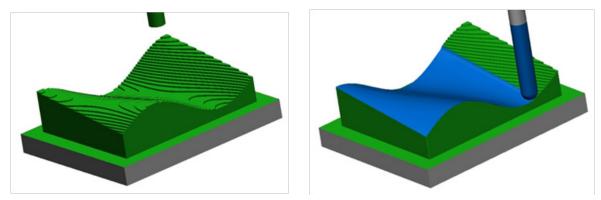

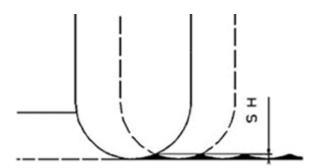**Fig. 6** Roughing (left) and finishing (right) operation

Fig. 7. SH (Scallop Height) - height inequality parameter setting

Measurement system

In the area of 3D measurement of machine parts, the 3D imaging devices are used thanks to their advantageous speed and accuracy. Portable coordinate measuring machine (CMM) FARO Arm was applied to measure two physical parts of freeform modeled in the CATIA environment. 3D non-contact measurement was used. Repeatability, based on working volume, was in the interval from 0.024 mm to 0.064 mm. In this case, the repeatability equaled to 0.034 mm. Measured clouds of points were saved in two separate files. The first file sc01.dat (containing 3 707 474 points) and the second one mr02.dat (containing 3 774 502 points). Loading these files into the Octave took about 23 seconds. After the transformation to the binary format, loading time has been reduced to about 0.5 second or even less.

WORKPIECE MANUFACTURING AND QUALITY CONTROL

In this section an algorithm for a measurement adjustment using a small workpiece coordinate system movement and rotation to achieve a

smaller least squares error of the produced surface for a given freeform surface defined by a function of two variables is considered.

Orthogonal distance

Let us consider a function

$$z = f(x,y), \quad (x,y) \in R \tag{3}$$

where: R denotes a rectangle $[0,l_x] \times [0,l_y]$ ($l_x > 0$ and $l_y > 0$ are the corresponding rectangle's sides lengths). Here we suppose that the function f(x,y) has continuous derivatives of the second order with respect to both variables.

Let us consider a "measured" point $P = (\hat{x}_p; \hat{y}_p; z_p)$ close to the surface S given as a graph of the function f(x,y), e.g.,

$$S = \{(x,y,f(x,y)) \,|\, (x,y) \in R\} \tag{4}$$

Our goal is to determine a projection P^S of the point P onto the surface S and the distance between the points P and P^S. So we are led to the minimization of the problem

$$\| P^S - P \|_2 = \min_{(x,y)} \| (x,y,f(x,y)) - (\hat{x}; \hat{y}_P; z_P) \|_2 \tag{5}$$

where $\| P^S - P \|_2$ denotes the Euclidean distance. Instead of the minimization of Eq. (5) we have minimized a square of the distance, hence we were looking for the minimum of the function

$$D^2(x,y) = (x - \hat{x}_P)^2 + (y - \hat{y}_P)^2 + (f(x,y) - z_P)^2 \tag{6}$$

We numerically solved a set of nonlinear equations for the stationary point (x_*, y_*) corresponding to the zero gradient of the function D^2:

$$(x_* - \hat{x}_P) + (f(x_*, y_*) - z_P) \cdot f'_x(x_*, y_*) = 0,$$
$$(y_* - \hat{y}_P) + (f(x_*, y_*) - z_P) \cdot f'_y(x_*, y_*) \tag{7}$$

using the Newton method [14]. This is equivalent to the minimization of D^2 by the Newton method [15]. In this case the Jacobian matrix for the system of nonlinear equations is equal to the Hessian matrix. Because the point (x_p, y_p) is supposed to be close to the point (x_*, y_*), two Newton iterations provided sufficient precision for approximation of the point (x_*, y_*). For approximation of projection, point P_2 has been used:

$$P^S \approx P_2 = (x_2, y_2, f(x_2, y_2)) \tag{8}$$

where $(x_0, y_0) = (\hat{x}_p; \hat{y}_p)$ has been used as an initial approximation for the Newton method.

Afterwards the orthogonal distance of the point P to the surface S has been approximated by

$$D(\hat{x}_P, \hat{y}_P, z_P) = \sqrt{(\hat{x}_P - x_2)^2 + (\hat{y}_P - y_2)^2 + (z_P - f(x_2, y_2))^2} \tag{9}$$

Minimization of the sum of squares of distances

Let set of measured points

$$
\begin{matrix}
x_{P1} & y_{P1} & z_{P1} \\
x_{P2} & y_{P2} & z_{P2} \\
\vdots & \vdots & \vdots \\
x_{PN} & y_{PN} & z_{PN}
\end{matrix}
\tag{10}
$$

of size N be given. If coordinates x_{Pi}, y_{Pi}, z_{Pi}, $i = 1,2, ..., N$ correspond to the coordinates x, y, and z of the graph above the rectangle R, then we need only to calculate the sum of distances squares to get the mean distance d_{mean}:

$$RSS = \sum_{i=1}^{N} D^2\left(x_{P_i}, y_{P_i}, z_{P_i}\right), \quad d_{\text{mean}} = \sqrt{\frac{RSS}{N}} \tag{11}$$

The RSS value is one of the characteristics of the workpiece production quality depending, however, on the number of points. Standard deviation d_{mean} can be used for the comparison of the precision for two points sets with the different numbers of points.

If we suppose that all points P_i are lying exactly on the surface, then evidently $d_{\text{mean}} = 0$. If, for any reason, the workpiece coordinate system will be displaced (moved in some direction and rotated in the (x, y) plane), then the measuring device will give us "surface points" which will not be laying on the surface, if we use the same coordinates in the workpiece coordinate system, and the mean distance value will be $d_{\text{mean}} > 0$. In that case we are able to recognize the workpiece coordinate system displacement by minimizing the value d_{mean} with respect to the possible shift and rotation.

We propose to apply the same idea in the case of a general measurement of the near-surface points. Suppose that the workpiece coordinate system origin O_w is located at the point (x_w, y_w) and the system is rotated by an angle α_w (see Fig. 8) with respect to the measuring device coordinate system. Then the "measured point" x- and y- coordinates are "tainted". We are looking for the values x_w, y_w and α_w. We define the optimal values x_w, y_w and α_w as the values, for which the RSS value for a given set of measured points is minimal.

We propose to apply the same idea in t α_w he case of a general measurement of the near-surface points. Suppose that the workpiece coordinate system origin O_w is located at the point (x_w, y_w) and the system is rotated by an angle α_w (see Fig. 8) with respect to the measuring device coordinate system.

Then the "measured point" x- and y- coordinates are "tainted". We are looking for the values x_w, y_w and α_w. We define the optimal values x_w, y_w and α_w as the values, for which the RSS value for a given set of measured points is minimal.

If we denote by $\tilde{P}_w$ the local "workpiece" coordinates of the projection $\tilde{P} = (x_p, y_p)$ of a point P onto the x–y plane, then we have

$$\tilde{P} = \mathcal{O}_w + R(\alpha) \cdot \tilde{P}_w, \quad \tilde{P}_w = R(-\alpha) \cdot (\tilde{P} - \mathcal{O}_w) \tag{12}$$

where R (α) is a rotation matrix for the angle α.

Hence, the true "workpiece" coordinates of the projection $\tilde{P}$ are then given by the following formulas

$$\hat{x}_P = (x_P - x_w) \cdot \cos \alpha_w + (y_P - y_w) \cdot \sin \alpha_w$$
$$\hat{y}_P = (y_P - y_w) \cdot \cos \alpha_w - (x_P - x_w) \cdot \sin \alpha_w \tag{13}$$

and we are indeed to determine the distance of the point $(\hat{x}_p; y_p; z_p)$ to the surface *S*. Thus the residual sum of squares depends on the values x_D, y_D and α_D:

$$RSS(x_D, y_D, \alpha_D) = \sum_{i=1}^{N} D^2\left(\hat{x}_{P_i}, \hat{y}_{P_i}, z_{P_i}\right) \tag{14}$$

and can be minimized with respect to these values.

For the minimization of the function (14) we were using the inexact Newton method based on the inexact gradient and the Hessian matrix [15] defined by the finite difference method. Point $O' = (x'_w, y'_w)$ (x'_w is the leftmost *x*-coordinate and y'_w is the smallest *y*-coordinate of all cloud points – see Fig. 8) for expected small angle α_w is serving as a good approximation of the origin O.

Further we will use (see Fig. 8)

$$x_w = x'_w + \Delta x_w, \quad y_w = y'_w + \Delta y_w \tag{15}$$

One two-dimensional and one three-dimensional Newton step have been sufficient to achieve good precision.

NUMERICAL RESULTS

Let us consider a function

$$f(x, y) = 15 + 10 \cdot \left[\left(1 - \frac{y}{80}\right) \cdot \cos\frac{\pi x}{50} - \frac{y}{80} \cdot \sin\frac{\pi x}{50}\right] \tag{16}$$
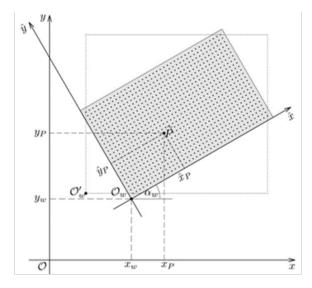
Fig. 8. Measurement device and workpiece coordinate systems

where: x ∈ [0, 100], y ∈ [0, 80] with units in mm. So therectangle *R* has the size 100 mm × 80 mm (see Fig. 9).

Below we will compare some results using the Nelder-Mead method [16] implemented in Octave with the results of the Newton method.

Using the Nelder-Mead method

Due to the large number of points and relatively slow computations in Octave only thousandth of points (step 1000) has been used for optimization. The results are shown in Table 1.

For computations an Octave function **fminsearch.m** written by S. Pelissier in 2006 has been used. It used a function **fmins.m** written by A. Adler in 2003 who modified for Octave the function **nmsmax.m** written by N.J. Higham [17], [18] in 2002.

During the optimization 111 function evaluations have been performed for **sc01.dat** and 114 for **mr02.dat**.

From experiments it is obvious, that the quality is much better after the location and rotation of the measurement device coordinate system – using the origin O'$_w$ leads to much more pessimistic estimation of the mean "error". All characteristics were better for the data **mr02.dat**.

Using the inexact Newton method

For the inexact Newton method applications based on the finite difference approximation of partial derivatives different approaches have been compared. From the point of view of the computational time, the best performance has been achieved using one two-dimensional Newton step for Δx_w and y_w approximation without the rotation, and next one three-dimensional Newton step for (Δx_w, y_w, α_w) and approximation. Moreover, the evaluation of the inexact gradient and Hessian matrix has been "optimized" using a common function.

The results for (Δx_w, y_w, $\alpha_w = 0, 0, 0$) given in Table 2 are the same as in Table 1, and are not shown here. The first part of Table 2 refers to the results of the first two-dimensional Newton step which uses 11 functional value evaluations, and which is approximately two times faster than one three-dimensional Newton step which uses 20 functional value evaluations.

Here we can see that the first two-dimensional step will supply the main improvement of the measurement results interpretation. Therefore, the second step can be omitted if we have no time for its realization. The C++ implementation of the program is much faster than the Octave implementation. The speedup for the smaller problems is about 800, for the full set of points the speedup is about 41.
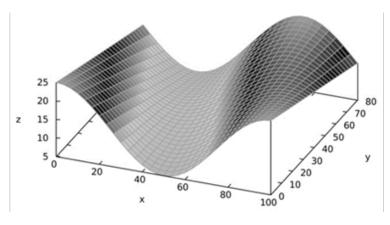

Fig. 9. Free-form surface represented by the function (16)

Table 1. Adjustment using the Nelder-Mead method

	sc01.dat	sc02.dat
$(\Delta x_w, y_w, \alpha_w)$	(0,0,0)	(0,0,0)
Mean surface distance [mm]	0.2786	0.30286
Max. positive offset [mm]	0.48074	0.51429
Max. negative offset [mm]	−0.44981	−0.51977
$(\Delta x_w, y_w, \alpha_w)$	(0.7167,0.4973,0.0804)	(0.7617,0.5299,−0.0314)
Mean surface distance [mm]	0.055142	0.024572
Max. positive offset [mm]	0.17997	0.080997
Max. negative offset [mm]	−0.15617	−0.12394
Total computation time [s]	149.83	157.31
Points number	3 708	3 775

Table 2. Adjustment using the inexact Newton method

	sc01.dat	sc02.dat
$(\Delta x_w, y_w, \alpha_w)$	(0.6630,0.5511,0)	(0,0,0)
Mean surface distance [mm]	0.0565	0.30223
Max. positive offset [mm]	0.17999	0.57223
Max. negative offset [mm]	−0.15741	−0.62206
Computation time [s]	1433.76	1438.02
$(\Delta x_w, y_w, \alpha_w)$	(0.7169,0.4973,0.0803)	(0.7166,0.5300,0.0314)
Mean surface distance [mm]	0.055142	0.024572
Max. positive ofset [mm]	0.17997	0.080928
Max. negative offset [mm]	−0.15617	−0.12384
Total computation time [s]	14.595+27.151=41.746	14.867+27.434=42.301
C++ computation time [s]	0.0208+0.0331=0.0539	0.0194+0.0313=0.0507
Points number	3 708	3 775

Table 3. Measurement results interpretation for the whole cloud with and without the workpiece coordinate system adjustment

	sc01.dat	sc02.dat
$(\Delta x_w, y_w, \alpha_w)$	(0,0,0)	(0,0,0)
Mean surface distance [mm]	0.27896	0.30223
Max. positive offset [mm]	0.93423	0.57223
Max. negative offset [mm]	−0.57223	−0.62206
Computation time [s]	1433.76	1438.02
$(\Delta x_w, y_w, \alpha_w)$	(0.7169,0.4973,0.0803)	(0.7616,0.5300,0.0314)
Mean surface distance [mm]	0.055683	0.024977
Max. positive ofset [mm]	0.59395	0.23678
Max. negative offset [mm]	−0.19518	−0.23627
Computation time [s]	1421.13	1457.85
C++ computation time [s]	12.247+22.480=34.727	12.453+22.771=35.524
Points number	3 707 474	3 774 502

CONCLUSION

Methods that are used for the evaluation of the form of the workpiece apply a best-fit criterion. Its biggest disadvantage is its use in cases of more significant form deviations. The proposed algorithm deals with this disadvantage and offers a way to solve this problem.

In Table 3 the results for all cloud points with the workpiece coordinate system origin placed at the point O'_w are compared with the results with an adjusted workpiece coordinate system.

One can see that the mean surface distance after the optimal adjustment for the whole cloud is just the same as the value for only thousandth of all points. The maximal positive and negative displacements for all cloud points are, of course, worse than the displacements for only part of the points. However, it is evident that the results – both the mean and maximal offsets – without the coordinate system adjustment are much more pessimistic.

REFERENCES

1. Ohara M., Higashi M. Integration of CAD/CAM systems in automotive body engineering. Computers & Graphics, 7 (3–4), 1983, 307–311, 313–314.

2. Mehrad V., Xue D., Gu P., Prediction of surface reconstruction uncertainties for freeform surface inspection. Measurement, 46 (8), 2013, 2682–2694.

3. Sitnik R., Błaszczyk P. M. Segmentation of unsorted cloud of points data from full field optical measurement for metrological validation. Computers in Industry, 63 (1), 2012, 30–44.

4. Oe T., Shizuki B., Tanaka J. Scan modeling: 3D modeling techniques using cross section of a shape. Proc. of 10th Asia Pacific Conference on Computer Human Interaction, New York, USA 2012, 243–250.

5. Kruth J.-P., Kerstens A. Reverse engineering modelling of freeform surfaces from point clouds subject to boundary conditions. Journal of Materials Processing Technology, 76 (1–3), 1998, 120–127.

6. Wu N., Yang C., Guo R., Zhang Z., Zhou C., Chen W., Tao L. Reverse Design and Manufacture of the Car Door Using Reverse Engineering Methods. American Society of Civil Engineers, 2011, ch. 384, 3849–3854.

7. Ochiai Y., Sekiya T. Generation of free-form surface in CAD for dies. Advances in Engineering Software, 22 (2), 1995, 113–118.

8. Lo C.-C. CNC machine tool surface interpolator for ball-end milling of free-form surfaces. International Journal of Machine Tools and Manufacture, 40 (3), 2000, 307–326.

9. Wei E.-J., Lin M.-C. Study on general analytical method for CNC machining the free-form surfaces. Journal of Materials Processing Technology, 168 (3), 2005, 408–413.

10. Sacharow A., Odendahl S., Peuker A., Biermann D., Surmann T., Zabel A. Iterative, simulation-based shape modification by free-form deformation of the NC programs. Advances in Engineering Software, 56 (2013), 63–71.

11. Zhang A. M., Fang D. Y., Qiu Y. Research and practice on new measuring and drafting mode of mechanical drawing based on reverse engineering. Measurement Technology and its Application: Applied Mechanics and Materials, 239, 2013, 645–648.

12. Lee R.-T., Shiou F.-J. Multi-beam laser probe for measuring position and orientation of freeform surface. Measurement, 44 (1), 2011, 1–10.

13. Kale K. B., Gurumoorthy B. Profile tolerance verification for free-form surfaces using medial axis transform. Proc. of 12th CIRP Conference on Computer Aided Tolerancing, 2013, 133–141.

14. Wait R. The Numerical Solution of Algebraic Equations. John Wiley & Sons, 1979.

15. Nocedal J., Wright S. Numerical optimization. Springer-Verlag, 1999.

16. Bunday B. D. Basic Optimisation Methods. Edward Arnold, 1984.

17. Higham N. J. Optimization by direct search in matrix computations. SIAM Journal on Matrix Analysis and Applications, 14 (2), 1993, 317–333.

18. Kelley C. T. Iterative Methods for Optimization. Frontiers in Applied Mathematics, Society for Industrial and Applied Mathematics, 1999.

19. Molnár V., Fedorko G., Stehlíková B., Michalik P.,

Kopas M. Mathematical models for indirect measurement of contact forces in hexagonal idler housing of pipe conveyor. Meas. J. Int. Meas. Confed., 47, 2014, 794–803.

20. Debski H., Teter A., Kubiak T., Samborski S. Local buckling, post-buckling and collapse of thin-walled channel section composite columns subjected to quasi-static compression. Compos. Struct., 136, 2016.

21. Garbacz T., Jachowicz T., Gajdoš I., Kijewski G. Research on the influence of blowing agent on selected properties of extruded cellular products. Adv. Sci. Technol. Res. J. 28 (9), 2015, 81-88.

22. Kráľ J.jr, Kráľ J. Verification of a three axis milling machine accuracy in the process of complex shaped part production. Applied Mechanics and Materials: Novel Trends in Production Devices and Systems. 474, 2014, 261-266.

23. Fedorko G., Kráľ J.jr, Kráľ J., Ristovic I., Molnár V. Determination of calculation for the shape of blades trace in the concrete mixer truck. Procedia Technology, 19, 2015, 395–401.

24. Kulka J., Mantic M., Fedorko G., Molnár V. Analysis of crane track degradation due to operation. Engineering Failure Analysis, 59, 2016, 384–395.